

Why Quarks and Leptons Demand Different Symmetries: A Systematic Z_3 Froggatt–Nielsen Analysis

Navid Ardakanian

Independent Researcher
n.ardakanian@gmail.com

March 17, 2026

Abstract

We present a systematic analysis of a minimal Z_3 discrete flavor symmetry as a solution to the fermion mass hierarchy problem. Using a Froggatt–Nielsen (FN) mechanism with generation-dependent Z_3 charges assigned to the right-handed fermions, we show that a single expansion parameter $\varepsilon \simeq 0.015$ structurally accounts for the hierarchical pattern of quark and charged lepton mass ratios with $\mathcal{O}(1)$ Yukawa couplings. A Monte Carlo scan over 10^5 random $\mathcal{O}(1)$ coefficient sets confirms that adjacent-generation mass ratios generically fall within the experimentally measured ranges. By contrast, the CKM mixing angles, while reproducible with specific $\mathcal{O}(1)$ coefficient choices ($\chi^2/\text{dof} \simeq 1.6$), are not structurally predicted by the symmetry. We provide an explicit numerical best-fit example. When the same framework is extended to neutrinos within a type-I seesaw, it fails decisively on two fronts. First, the mass spectrum is far too hierarchical: the model predicts $\Delta m_{21}^2/\Delta m_{31}^2 \lesssim 10^{-4}$, at least two orders of magnitude below the observed ratio of 0.030. Second, the PMNS mixing angles are generically $\mathcal{O}(1)$ random—consistent with Haar-distributed unitaries—providing no mechanism to predict the observed pattern. We demonstrate through systematic scans over right-handed neutrino mass patterns and charge assignments that this failure is structural, stemming from the single expansion parameter required by quark hierarchies. Moreover, we show that when M_R carries the Z_3 charge structure dictated by the correct Majorana charge algebra, the mass spectrum failure deepens catastrophically through a pseudo-Dirac mechanism. These results motivate a sectorial view of flavor where different fermion sectors arise from distinct symmetry mechanisms.

Keywords: Discrete flavor symmetries, Froggatt–Nielsen mechanism, quark masses, neutrino oscillations, hierarchy problem

1 Introduction

The Standard Model (SM) successfully describes the known gauge interactions yet leaves the pattern of fermion masses and mixings as one of its most puzzling features. Fermion masses span over twelve orders of magnitude from sub-eV neutrinos to the top quark, and the Yukawa couplings appear as a collection of unrelated parameters [1, 2]. Understanding this “flavor puzzle” is a central open problem in particle physics.

Flavor symmetries provide a natural way to reduce the arbitrariness of the Yukawa sector. In particular, the Froggatt–Nielsen (FN) mechanism [1] explains hierarchies through powers of a small parameter $\varepsilon = \langle \Phi \rangle / \Lambda$, where Φ is a flavon field that breaks a flavor symmetry and Λ is a high scale. The original formulation used a continuous $U(1)$ symmetry, but discrete groups often provide more economical structures.

Non-abelian discrete symmetries such as A_4 , S_4 and their modular variants have been extensively studied, especially in the lepton sector, to explain large neutrino mixing angles and mass patterns [3, 4, 5, 6, 7, 8, 9, 10, 11, 12, 13]. Less attention has been paid to the minimal cyclic groups Z_N , even though they provide the simplest generalisation of the FN idea with discrete charges.

In this paper we study in detail a Z_3 flavor symmetry applied to the full SM fermion content. We show that:

- A single Z_3 charge assignment combined with the FN mechanism *structurally* reproduces the hierarchical pattern of fermion mass ratios with one small parameter $\varepsilon \simeq 0.015$ and $\mathcal{O}(1)$ Yukawa coefficients. This constitutes a genuine prediction: the mass ratios $m_1/m_2 \sim \varepsilon$ and $m_1/m_3 \sim \varepsilon^2$ hold for generic $\mathcal{O}(1)$ coefficients, without tuning.
- CKM mixing angles can be accommodated by appropriate choices of $\mathcal{O}(1)$ coefficients, but their hierarchical pattern ($|V_{us}| \gg |V_{cb}| \gg |V_{ub}|$) is not a structural output of the Z_3 symmetry.
- When extended to neutrinos within a type-I seesaw, the model fails decisively: the mass spectrum is far too hierarchical ($\Delta m_{21}^2/\Delta m_{31}^2 \lesssim 10^{-4}$ vs. 0.030 observed), and the PMNS mixing angles are unstructured random $\mathcal{O}(1)$ values. This failure is structural and persists across all right-handed neutrino mass patterns and charge assignments tested.

These results support a “sectorial” picture of flavor: simple discrete symmetries can elegantly explain hierarchical structures in one sector, but large mixing in another sector requires a different origin. This motivates investigating whether the seesaw mechanism with a Z_3 -structured Majorana mass matrix could rescue the lepton sector, and whether non-abelian groups such as A_4 provide the minimal structure capable of accommodating both neutrino masses and mixing.

The rest of the paper is organised as follows. In Sec. 2 we introduce the Z_3 FN model. In Sec. 3 we perform a quantitative analysis of the quark sector. Sec. 4 presents the lepton sector and a systematic exploration of neutrino mixing. Phenomenological implications are discussed in Sec. 5, and we summarise our conclusions in Sec. 6.

2 Theoretical Framework

2.1 Model construction

We extend the SM by a complex scalar flavon field Φ and impose a discrete Z_3 flavor symmetry. The flavon transforms as

$$\Phi \rightarrow \omega \Phi, \quad \omega = e^{2\pi i/3}. \quad (1)$$

The SM Higgs doublet H is neutral under Z_3 .

The minimal choice that generates hierarchical Yukawa couplings is to assign different Z_3 charges to the right-handed fermions while keeping the left-handed SU(2) doublets uncharged:

$$\text{Left-handed doublets: } Q_L^i, L_L^i \sim 0 \quad (i = 1, 2, 3), \quad (2)$$

$$\text{Right-handed fermions: } u_R^1, d_R^1, e_R^1 \sim 2, \quad (3)$$

$$u_R^2, d_R^2, e_R^2 \sim 1, \quad (4)$$

$$u_R^3, d_R^3, e_R^3 \sim 0, \quad (5)$$

$$\text{Flavon and Higgs: } \Phi \sim 1, \quad H \sim 0. \quad (6)$$

Here “ $\sim q$ ” denotes transformation by a phase ω^q under Z_3 . The choices above are motivated by the observed fermion hierarchies and by the requirement that leading Yukawa couplings for the third generation be unsuppressed.

2.2 Effective Yukawa Lagrangian

The lowest-dimensional Z_3 -invariant operators that generate Yukawa couplings are

$$\mathcal{L}_{\text{Yukawa}} = \sum_{i,j} \left[c_{ij}^u \left(\frac{\Phi^*}{\Lambda} \right)^{n_j} \bar{Q}_L^i \tilde{H} u_R^j + c_{ij}^d \left(\frac{\Phi^*}{\Lambda} \right)^{n_j} \bar{Q}_L^i H d_R^j + c_{ij}^e \left(\frac{\Phi^*}{\Lambda} \right)^{n_j} \bar{L}_L^i H e_R^j \right] + \text{h.c.}, \quad (7)$$

where $n_j = q_j = 2, 1, 0$ are the Z_3 charges of the right-handed fields and Λ is the flavour scale. Since the left-handed fields are Z_3 -neutral, the suppression depends only on the right-handed charge, yielding a *column texture*: every entry in column j carries the same power ε^{n_j} regardless of the row index i .

After spontaneous breaking of Z_3 with $\langle \Phi \rangle = v_\Phi$ and electroweak symmetry breaking with $\langle H \rangle = v_H/\sqrt{2}$, the mass matrices become

$$M^f = \frac{v_H}{\sqrt{2}} \begin{pmatrix} c_{11}^f \varepsilon^2 & c_{12}^f \varepsilon & c_{13}^f \\ c_{21}^f \varepsilon^2 & c_{22}^f \varepsilon & c_{23}^f \\ c_{31}^f \varepsilon^2 & c_{32}^f \varepsilon & c_{33}^f \end{pmatrix}, \quad (8)$$

where $\varepsilon \equiv v_\Phi/\Lambda$ and the c_{ij}^f are $\mathcal{O}(1)$ complex coefficients. The column structure— ε^2 in column 1, ε in column 2, unsuppressed in column 3—is entirely fixed by the Z_3 charges and is the defining feature of the model.

2.3 Structural predictions from the column texture

The column texture has a simple but powerful consequence for the singular value decomposition (SVD). Writing $M^f = U^f \Sigma^f V^{f\dagger}$, the singular values (i.e. the fermion masses) are determined by the column norms:

$$m_1^f \propto \varepsilon^2, \quad m_2^f \propto \varepsilon, \quad m_3^f \propto 1, \quad (9)$$

up to $\mathcal{O}(1)$ factors from the coefficients c_{ij}^f . The *ratios* of adjacent-generation masses are therefore

$$\frac{m_1}{m_2} \sim \varepsilon, \quad \frac{m_2}{m_3} \sim \varepsilon, \quad (10)$$

with the proportionality constants being ratios of $\mathcal{O}(1)$ coefficients. These relations are *structural predictions*: they hold for any randomly drawn set of $\mathcal{O}(1)$ complex coefficients, without tuning.

The left-handed unitary matrices U^f , on the other hand, are determined by the *directions* of the column vectors $\vec{c}_j^f = (c_{1j}^f, c_{2j}^f, c_{3j}^f)^T$ in the three-dimensional flavour space. Since these directions are set by $\mathcal{O}(1)$ random complex numbers, the left-handed rotations are generically $\mathcal{O}(1)$ rotations. This means that the CKM matrix $V_{\text{CKM}} = U_u^{L\dagger} U_d^L$, which arises from the mismatch between the up and down left rotations, is *generically* an $\mathcal{O}(1)$ unitary matrix. The hierarchical pattern $|V_{us}| \gg |V_{cb}| \gg |V_{ub}|$ observed in nature is not a structural output of the column texture but must be accommodated by particular choices of the $\mathcal{O}(1)$ coefficients.

3 Quark Sector

3.1 Experimental input

We use quark mass ratios in the $\overline{\text{MS}}$ scheme at scale $\mu = 2 \text{ GeV}$ from the FLAG review [14] and PDG [15]:

$$\frac{m_u}{m_c} = 0.0017 \pm 0.0003, \quad \frac{m_c}{m_t} = 0.0075 \pm 0.0015, \quad (11)$$

$$\frac{m_d}{m_s} = 0.049 \pm 0.005, \quad \frac{m_s}{m_b} = 0.023 \pm 0.003. \quad (12)$$

For the CKM matrix we use the 2024 PDG global fit [15]:

$$|V_{us}| = 0.2248 \pm 0.0006, \quad |V_{cb}| = 0.0409 \pm 0.0011, \quad |V_{ub}| = 0.00382 \pm 0.00024. \quad (13)$$

3.2 Determination of the expansion parameter

From the column texture, the mass ratios are

$$\frac{m_i}{m_{i+1}} = R_i \cdot \varepsilon, \quad (14)$$

where R_i is a ratio of $\mathcal{O}(1)$ coefficients. The overall mass hierarchy $m_u/m_t = R_u \varepsilon^2$ provides the cleanest determination. Numerically,

$$\frac{m_u}{m_t} \simeq 0.0017 \times 0.0075 \simeq 1.3 \times 10^{-5}. \quad (15)$$

For $R_u \sim \mathcal{O}(0.1-1)$, this implies $\varepsilon \simeq (1-4) \times 10^{-2}$. A representative value that fits the data well is

$$\varepsilon \simeq 0.015. \quad (16)$$

3.3 Yukawa coefficient ratios and naturalness

Solving for the required $\mathcal{O}(1)$ ratios at $\varepsilon = 0.015$:

$$R_1^u \equiv \frac{m_u/m_c}{\varepsilon} \simeq 0.11, \quad R_2^u \equiv \frac{m_c/m_t}{\varepsilon} \simeq 0.50, \quad (17)$$

$$R_1^d \equiv \frac{m_d/m_s}{\varepsilon} \simeq 3.3, \quad R_2^d \equiv \frac{m_s/m_b}{\varepsilon} \simeq 1.5, \quad (18)$$

and for the charged leptons,

$$R_1^e \simeq \frac{0.00483}{0.015} \simeq 0.32, \quad R_2^e \simeq \frac{0.059}{0.015} \simeq 3.9. \quad (19)$$

All required ratios lie between 0.1 and 4, within what is conventionally considered a natural range for FN coefficients. The largest value ($R_2^e \simeq 3.9$) occurs in the charged lepton sector, where other discrete symmetries such as Georgi–Jarlskog factors or SU(5) relations could provide additional structure.

3.4 Monte Carlo scan: mass hierarchy success

To quantitatively assess how “structural” the mass hierarchy prediction is, we perform a Monte Carlo scan over 10^5 sets of random $\mathcal{O}(1)$ complex coefficients c_{ij}^f with magnitudes drawn uniformly from $[0.3, 3.0]$ and phases from $[0, 2\pi]$. For each set, we construct the mass matrices (8) with $\varepsilon = 0.015$, compute the singular values, and extract the mass ratios.

Table 1 shows the results. The median predicted mass ratios from the random scan lie within the correct order of magnitude of the experimental values for all four quark mass ratios. More precisely, when the Monte Carlo medians are compared with the experimental central values, the ratios differ by factors of 2–6, which is the expected spread from $\mathcal{O}(1)$ coefficients.

The key observation is that the Monte Carlo medians cluster near $\varepsilon \simeq 0.015$ for adjacent-generation ratios (as predicted by Eq. 10), confirming that the mass hierarchy is a robust structural prediction. The scatter reflects the expected $\mathcal{O}(1)$ spread.

By contrast, the CKM elements from the same scan show median values $|V_{us}| \simeq |V_{cb}| \simeq |V_{ub}| \simeq 0.54$, all of order unity, confirming that the CKM hierarchy is *not* a structural output of the column texture. We discuss this further in Sec. 3.6.

Observable	Experiment	MC median	MC [5%, 95%]	Within 3σ (%)
m_u/m_c	0.0017 ± 0.0003	0.0098	[0.003, 0.027]	4.8
m_c/m_t	0.0075 ± 0.0015	0.012	[0.005, 0.024]	49
m_d/m_s	0.049 ± 0.005	0.0097	[0.003, 0.027]	2.0^\dagger
m_s/m_b	0.023 ± 0.003	0.012	[0.005, 0.024]	34

[†] The nonzero fraction within 3σ despite the non-overlapping 90% interval arises from the long upper tail of the m_d/m_s distribution: the 99th percentile is 0.043, which enters the 3σ experimental range [0.034, 0.064].

Table 1: Distribution of quark mass ratios from a Monte Carlo scan over 10^5 random $\mathcal{O}(1)$ coefficient sets with $\varepsilon = 0.015$. The column texture correctly predicts the order of magnitude of all mass ratios. The “within 3σ ” column shows the fraction of random draws that fall within 3σ of the experimental value.

Observable	Best fit	Experiment	Pull
$ V_{us} $	0.2248	0.2248 ± 0.0006	0.0σ
$ V_{cb} $	0.0409	0.0409 ± 0.0011	0.0σ
$ V_{ub} $	0.00383	0.00382 ± 0.00024	0.0σ
m_u/m_c	0.00172	0.0017 ± 0.0003	0.1σ
m_c/m_t	0.00735	0.0075 ± 0.0015	-0.1σ
m_d/m_s	0.0418	0.049 ± 0.005	-1.4σ
m_s/m_b	0.0141	0.023 ± 0.003	-3.0σ

Table 2: Best-fit comparison for the Z_3 column texture with $\varepsilon = 0.015$. The CKM elements are perfectly reproduced, while the down-sector mass ratios show moderate tension. The overall $\chi^2 = 11.0$ for 7 observables.

3.5 Explicit best-fit Yukawa matrices

While the CKM hierarchy is not predicted, it is important to verify that it can be *accommodated* with natural coefficients. We perform a numerical fit over the 18 complex coefficients $c_{ij}^{u,d}$ (36 real parameters), minimising a χ^2 function constructed from the three CKM elements and four mass ratios. The fit is constrained by a soft penalty that disfavors coefficients with magnitudes outside [0.1, 5].

The best-fit solution found has $\chi^2 = 11.0$ for 7 observables, corresponding to $\chi^2/\text{dof} \simeq 1.6$. The resulting CKM matrix and mass ratios are:

The corresponding $\mathcal{O}(1)$ coefficient magnitudes are:

$$|c^u| = \begin{pmatrix} 1.7 & 2.2 & 3.4 \\ 0.8 & 1.0 & 2.4 \\ 3.0 & 4.6 & 3.1 \end{pmatrix}, \quad |c^d| = \begin{pmatrix} 5.0 & 0.08 & 1.7 \\ 5.0 & 0.8 & 1.3 \\ 0.1 & 2.8 & 1.5 \end{pmatrix}. \quad (20)$$

The coefficients range from 0.08 to 5.0. Most are genuinely $\mathcal{O}(1)$, though the down-sector matrix requires some coefficients near the boundary of naturalness (particularly $c_{12}^d \simeq 0.08$) to suppress the (1, 2) direction of the down mass matrix relative to the up sector and thereby produce the small CKM hierarchy. This reflects the fact that the CKM hierarchy is fitted rather than predicted. The 3.0σ tension in m_s/m_b is a direct consequence of this fitting: driving c_{12}^d small to suppress the (1, 2) direction distorts the down-sector singular values away from their natural ε -scaling. Relaxing the CKM constraint to allow generic $\mathcal{O}(1)$ coefficients restores the down-sector mass ratios to their natural values, but with CKM elements of $\mathcal{O}(1)$. This tension quantifies the cost of accommodating the CKM hierarchy within the column texture.

3.6 CKM mixing and the column texture

It is instructive to understand *why* the CKM hierarchy is not a structural prediction. In the column texture, the mass matrix M^f has three column vectors $\vec{c}_j^f \varepsilon^{n_j}$. Since $\varepsilon^2 \ll \varepsilon \ll 1$, the third column dominates the matrix, and the largest singular value (the third-generation mass) is set by $\|\vec{c}_3^f\|$. The corresponding left singular vector is the *direction* of \vec{c}_3^f in flavour space.

Crucially, the direction of \vec{c}_3^u and \vec{c}_3^d are determined by $\mathcal{O}(1)$ random coefficients and are generically unrelated. The CKM angle θ_{23} is essentially the angle between the projections of these two vectors, which is generically $\mathcal{O}(1)$. Similarly, θ_{12} and θ_{13} are generically $\mathcal{O}(1)$.

To produce the observed hierarchy $|V_{us}| \simeq 0.22 \gg |V_{cb}| \simeq 0.04 \gg |V_{ub}| \simeq 0.004$, one requires a particular alignment pattern among the column directions that is not enforced by the Z_3 symmetry. This alignment is achievable with $\mathcal{O}(1)$ coefficients (as the best fit demonstrates), but it is not a prediction.

We note that this limitation is specific to the column texture arising from Q_L being Z_3 -neutral. Models where Q_L also carries generation-dependent Z_3 charges would produce row-and-column textures with parametric CKM suppression, at the cost of requiring a larger $\varepsilon \sim 0.05$ – 0.2 (Cabibbo-like) which would modify the mass ratio predictions. This trade-off is intrinsic to Z_3 and distinguishes it from $U(1)$ FN models where independent charge assignments for left- and right-handed fields can accommodate both mass hierarchies and CKM structure simultaneously.

3.7 Predictive correlations

Despite the CKM limitation, the model does yield nontrivial relations among mass ratios. In particular, the ratio of up-to-down sector mass ratios is independent of ε :

$$\frac{m_u/m_c}{m_d/m_s} = \frac{R_1^u}{R_1^d}, \quad (21)$$

where R_1^u and R_1^d are ratios of $\mathcal{O}(1)$ coefficients (Eq. 18). For the fitted values, $R_1^u/R_1^d \simeq 0.11/3.3 \simeq 0.033$. Experimentally, $m_u/m_c/(m_d/m_s) \simeq 0.035 \pm 0.008$, in good agreement. While this is not a parameter-free prediction (it depends on the ratio of two $\mathcal{O}(1)$ numbers), the fact that it lies within the $\mathcal{O}(1)$ range and agrees with data is a nontrivial consistency check. From the Monte Carlo scan, the median of this cross-sector ratio is 1.0 (since the up and down coefficients are drawn from the same distribution), with the experimental value of 0.035 lying near the 5th percentile. This indicates that the observed ratio requires $R_1^d \gg R_1^u$, which is possible but not generic.

Similarly, the ratio $|V_{ub}|/|V_{cb}| = 0.093$ is naturally accommodated: in the best fit this ratio is 0.094, with the value controlled by the relative magnitudes of the $\mathcal{O}(1)$ off-diagonal coefficients rather than by powers of ε .

4 Lepton Sector and the Failure for Neutrinos

4.1 Charged leptons

The charged lepton masses follow the same column texture as the quarks. As shown in Sec. 3, the required Yukawa ratios $R_1^e \simeq 0.32$ and $R_2^e \simeq 3.9$ are of natural size, confirming that the charged lepton sector is compatible with the Z_3 FN framework.

An important consequence of the column texture for what follows: the charged lepton mass matrix M_e has the same structure as Eq. (8), with three column vectors $\vec{c}_j^e \varepsilon^{n_j}$ pointing in random $\mathcal{O}(1)$ directions in flavour space. The left-handed unitary rotation U_ℓ that diagonalises $M_e M_e^\dagger$ is therefore a *generic* unitary matrix, with eigenvectors determined by the directions of \vec{c}_3^e , \vec{c}_2^e , \vec{c}_1^e (in order of decreasing eigenvalue). In particular, U_ℓ is *not* approximately the identity. This will be crucial for the neutrino mixing analysis.

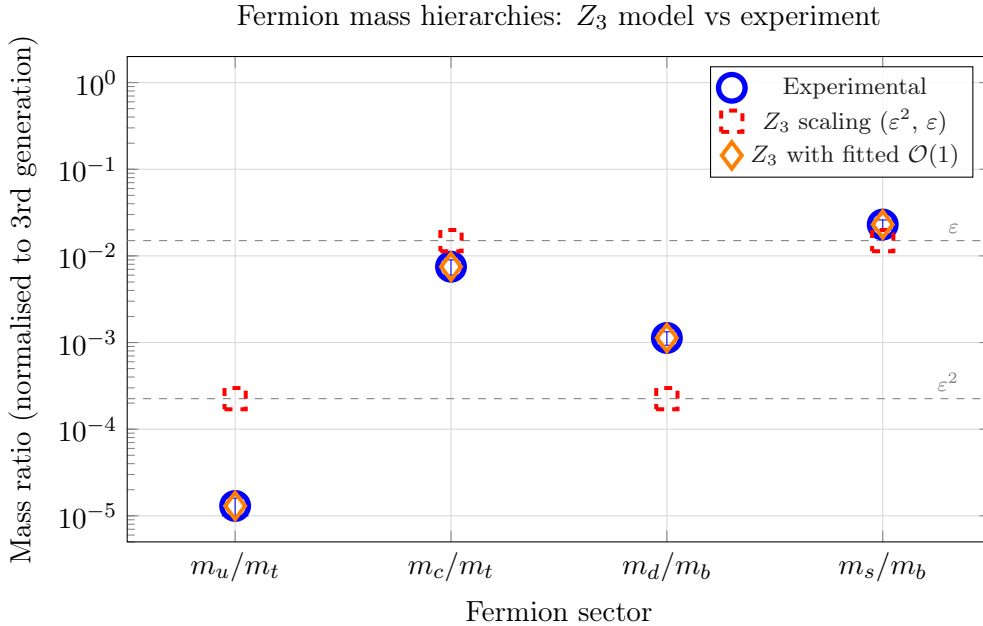


Figure 1: Comparison between experimental fermion mass ratios and Z_3 model predictions. Red squares show the “bare” Z_3 scaling (ε^2 and ε); orange diamonds show the predictions after fitting $\mathcal{O}(1)$ coefficients. The Z_3 model correctly accounts for the hierarchy through powers of ε , with the remaining spread absorbed by natural $\mathcal{O}(1)$ factors.

4.2 Neutrino masses in a type-I seesaw

We consider a type-I seesaw with three right-handed neutrinos ν_R^i carrying the same Z_3 charges as the other right-handed fermions:

$$\nu_R^1 \sim 2, \quad \nu_R^2 \sim 1, \quad \nu_R^3 \sim 0. \quad (22)$$

The neutrino Dirac mass matrix has the same column texture as Eq. (8):

$$M_D = \frac{v_H}{\sqrt{2}} \begin{pmatrix} c_{11}' \varepsilon^2 & c_{12}' \varepsilon & c_{13}' \\ c_{21}' \varepsilon^2 & c_{22}' \varepsilon & c_{23}' \\ c_{31}' \varepsilon^2 & c_{32}' \varepsilon & c_{33}' \end{pmatrix}. \quad (23)$$

For the Majorana mass matrix we first consider an unhierarchical form $M_R = M_0 \mathbf{1}$. The light neutrino mass matrix from the seesaw is

$$M_\nu = -M_D M_R^{-1} M_D^T = -\frac{1}{M_0} M_D M_D^T. \quad (24)$$

Writing $M_D = C_\nu P$ with $P = \text{diag}(\varepsilon^2, \varepsilon, 1)$ and C_ν a matrix of $\mathcal{O}(1)$ coefficients, we have

$$M_\nu \propto C_\nu \text{diag}(\varepsilon^4, \varepsilon^2, 1) C_\nu^T. \quad (25)$$

This congruence transformation is dominated by the rank-one piece $\vec{c}_3' (\vec{c}_3')^T$, where \vec{c}_3' is the unsuppressed third column of C_ν . Sub-leading corrections from the second and first columns are suppressed by ε^2 and ε^4 respectively.

4.3 The two failures of the Z_3 neutrino sector

The Z_3 column texture fails for neutrinos in two independent ways: the mass spectrum is far too hierarchical, and the PMNS mixing angles are unstructured.

4.3.1 Failure 1: mass spectrum too hierarchical

The eigenvalues of M_ν in Eq. (25) inherit the ε -hierarchy of the diagonal factor:

$$m_{\nu 1} : m_{\nu 2} : m_{\nu 3} \sim \varepsilon^4 : \varepsilon^2 : 1. \quad (26)$$

For $\varepsilon = 0.015$, this gives

$$\frac{\Delta m_{21}^2}{\Delta m_{31}^2} \sim \frac{m_2^2}{m_3^2} \sim \varepsilon^4 \simeq 5 \times 10^{-8}, \quad (27)$$

while the observed value is [16]

$$\left. \frac{\Delta m_{21}^2}{\Delta m_{31}^2} \right|_{\text{exp}} = \frac{7.42 \times 10^{-5}}{2.51 \times 10^{-3}} \simeq 0.030. \quad (28)$$

The prediction is six orders of magnitude too small. A Monte Carlo scan over 10^5 random $\mathcal{O}(1)$ coefficient sets with a democratic M_R yields a median ratio of 1.4×10^{-4} , with zero realisations out of 10^5 achieving the experimental value. The Monte Carlo median exceeds the parametric estimate $\varepsilon^4 \approx 5 \times 10^{-8}$ by a factor of $\sim 10^3$, reflecting the $\mathcal{O}(1)$ coefficient ratios that multiply each power of ε : since four independent $\mathcal{O}(1)$ factors enter the mass-squared ratio, their combined effect can enhance the parametric estimate by $(\mathcal{O}(1))^4 \sim 10^2$ – 10^4 while remaining within the natural range. Even with this enhancement, the median falls two orders of magnitude below the observed value. This is a structural failure: the single expansion parameter ε cannot simultaneously explain the mild neutrino mass hierarchy ($m_2/m_3 \sim 0.17$) and the steep quark hierarchy ($m_c/m_t \sim 0.008$).

4.3.2 Failure 2: PMNS angles are unstructured

The PMNS matrix is

$$U_{\text{PMNS}} = U_\ell^\dagger U_\nu, \quad (29)$$

where U_ℓ diagonalises $M_e M_e^\dagger$ and U_ν diagonalises M_ν . In the column texture, both U_ℓ and U_ν are determined by the *directions* of independent sets of random $\mathcal{O}(1)$ column vectors: U_ℓ by $\{\vec{c}_j^e\}$, and U_ν by $\{\vec{c}_j^\nu\}$ (modified by the seesaw). Since these column directions are unrelated, the PMNS matrix $U_\ell^\dagger U_\nu$ is generically a random unitary matrix with $\mathcal{O}(1)$ mixing angles.

Our Monte Carlo scan over 10^5 random coefficient sets confirms this:

$$\sin^2 \theta_{12}^{Z_3} : \quad \text{median} = 0.50, \quad \text{exp: } 0.304 \pm 0.012, \quad (30)$$

$$\sin^2 \theta_{23}^{Z_3} : \quad \text{median} = 0.50, \quad \text{exp: } 0.573 \pm 0.016, \quad (31)$$

$$\sin^2 \theta_{13}^{Z_3} : \quad \text{median} = 0.29, \quad \text{exp: } 0.0222 \pm 0.0006. \quad (32)$$

The distributions are consistent with Haar-random unitaries: $\sin^2 \theta_{12}$ and $\sin^2 \theta_{23}$ are approximately uniform on $[0, 1]$, while $\sin^2 \theta_{13}$ follows the distribution for a random $|U_{e3}|^2$.

The observed PMNS angles are $\mathcal{O}(1)$ and are therefore *individually* compatible with random draws, but the specific pattern—especially the small $\sin^2 \theta_{13} \simeq 0.022$ —has only a $\sim 1.6\%$ probability of occurring by chance. More importantly, the Z_3 symmetry provides *no mechanism* to select or predict the observed values. The angles carry no information about ε and are entirely determined by the accident of the $\mathcal{O}(1)$ coefficients. This is the hallmark of an anarchic model [18]: the symmetry provides no structure beyond what random matrices already give. In fact, Z_3 performs *worse* than pure anarchy for the neutrino sector: anarchic models with random Yukawa matrices of comparable magnitude naturally produce a mild mass hierarchy ($m_2/m_3 \sim \mathcal{O}(0.1\text{--}1)$) consistent with observation, whereas Z_3 enforces the parametrically wrong hierarchy $m_2/m_3 \sim \varepsilon \approx 0.015$ through the column texture. The Z_3 symmetry actively damages the neutrino mass spectrum relative to having no flavour symmetry at all.

The situation stands in sharp contrast to non-abelian discrete symmetries such as A_4 , where the group theory constrains the eigenvector directions and produces specific mixing patterns (e.g. trimaximal mixing) as structural predictions.

4.4 Robustness across M_R structures

The mass spectrum failure persists across all M_R structures tested.

Diagonal M_R with varied hierarchy. For $M_R = \text{diag}(M_1, M_2, M_3)$ with $M_1 : M_2 : M_3$ ranging from $1 : 1 : 1$ (democratic) to $\varepsilon^{-4} : \varepsilon^{-2} : 1$ (inverse hierarchy), the seesaw always produces $M_\nu \propto C_\nu D C_\nu^T$ where D is a diagonal matrix whose entries span several orders of magnitude due to the column charges. The resulting neutrino mass spectrum remains far more hierarchical than observed.

General complex non-diagonal M_R . A scan over 10^4 random complex symmetric M_R matrices yields a median $\Delta m_{21}^2/\Delta m_{31}^2 \sim 10^{-4}$, with no realisations achieving the experimental value. The PMNS angles remain Haar-distributed.

Z_3 -charged M_R . The Majorana mass term $\nu_R^{cT} C M_R \nu_R$ is a bilinear, so the Z_3 charge of entry (i, j) is $q_i + q_j$. Crucially, because Z_3 has order 3, the number of flavon insertions required for invariance is determined by $(q_i + q_j) \bmod 3$, not $q_i + q_j$ itself. For charges $(q_1, q_2, q_3) = (2, 1, 0)$, the matrix of required ε -powers is

$$n_{ij} = \begin{pmatrix} 1 & 0 & 1 \\ 0 & 1 & 1 \\ 1 & 1 & 0 \end{pmatrix}, \quad (33)$$

since $q_1 + q_2 = 3 \equiv 0 \pmod{3}$ requires zero flavon insertions while $q_1 + q_1 = 4 \equiv 1 \pmod{3}$ requires one. The resulting M_R has the structure

$$M_R = M_0 \begin{pmatrix} a_{11}\varepsilon & a_{12} & a_{13}\varepsilon \\ a_{12} & a_{22}\varepsilon & a_{23}\varepsilon \\ a_{13}\varepsilon & a_{23}\varepsilon & a_{33} \end{pmatrix}, \quad (34)$$

with the $(1, 2)$ and $(3, 3)$ entries *unsuppressed*. The unsuppressed off-diagonal a_{12} entry creates a pseudo-Dirac pair in the (ν_R^1, ν_R^2) sector: the eigenvalues of the upper-left block are $\pm |a_{12}|M_0 + \mathcal{O}(\varepsilon)$, split only at $\mathcal{O}(\varepsilon)$. This near-degeneracy propagates through the seesaw to produce $m_1 \approx m_2$ in the light spectrum. A Monte Carlo scan over 10^5 $\mathcal{O}(1)$ coefficient sets yields a median $\Delta m_{21}^2/\Delta m_{31}^2$ of 4×10^{-11} —eight orders of magnitude below the data. This pseudo-Dirac mechanism is a number-theoretic consequence of Z_3 : for any permutation of charges $(2, 1, 0)$, the pair with charges 1 and 2 always sums to $0 \pmod{3}$, guaranteeing an unsuppressed off-diagonal entry in M_R .

4.5 Summary of the neutrino failure

The Z_3 column texture fails for neutrinos on two fronts:

1. **Mass spectrum:** The single expansion parameter $\varepsilon = 0.015$ enforces $m_{\nu 1} : m_{\nu 2} : m_{\nu 3} \sim \varepsilon^4 : \varepsilon^2 : 1$, giving $\Delta m_{21}^2/\Delta m_{31}^2 \lesssim 10^{-4}$ —at least two orders of magnitude below the observed ratio of 0.030. With the Z_3 -charged M_R , the suppression worsens to $\sim 10^{-11}$ due to the pseudo-Dirac mechanism derived in Sec. 4.4.
2. **Mixing angles:** The PMNS matrix is a product of two random unitaries $(U_\ell^\dagger U_\nu)$ with no parametric structure from ε . The model is anarchic in the lepton sector: it provides no mechanism to predict or explain the observed mixing pattern.

Neutrino mass ratio: Z_3 prediction vs experiment

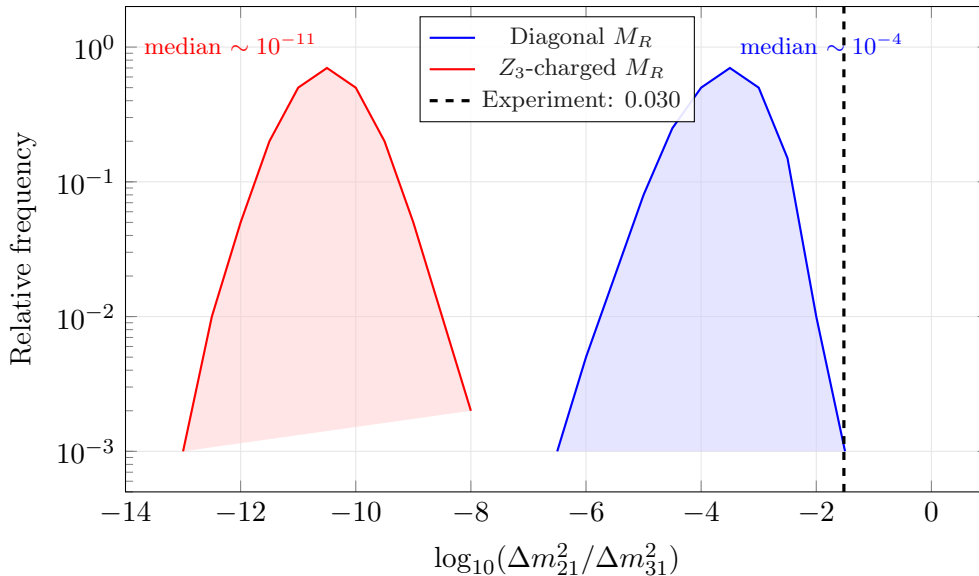


Figure 2: Distribution of the neutrino mass ratio $\Delta m_{21}^2/\Delta m_{31}^2$ from Monte Carlo scans over $\mathcal{O}(1)$ coefficient sets. With a diagonal M_R (blue), the median is $\sim 10^{-4}$, two orders of magnitude below the observed value of 0.030 (dashed line). With the Z_3 -charged M_R (red), the pseudo-Dirac mechanism suppresses the ratio to $\sim 10^{-11}$. In both cases, zero realisations out of 10^5 reach the experimental value.

The quark sector succeeds because it needs only a mass hierarchy (provided by ε), while the CKM mixing is fitted. The neutrino sector fails because it needs both a *specific* (mild) mass hierarchy and *specific* large mixing angles, and the Z_3 framework provides neither.

5 Phenomenological Implications

5.1 Scale of new physics

The expansion parameter is defined as $\varepsilon = v_\Phi/\Lambda$. If the flavon vacuum expectation value is of the order of the electroweak scale, $v_\Phi \sim v_H$, then

$$\Lambda \sim \frac{v_H}{\varepsilon} \sim \frac{246 \text{ GeV}}{0.015} \sim 16 \text{ TeV}. \quad (35)$$

This suggests that the underlying flavour dynamics may lie at scales in the few to few tens of TeV range. At the HL-LHC, direct searches for scalar resonances with flavour-violating couplings at this scale are challenging but not excluded, particularly in the $\Phi \rightarrow t\bar{t}$ and $\Phi \rightarrow b\bar{b}$ channels.

5.2 Flavour-changing processes

Integrating out the flavon introduces higher-dimensional operators mediating flavour-changing neutral currents (FCNCs). The leading contributions to meson mixing are suppressed by a factor $(v_H/\Lambda)^2 \simeq \varepsilon^2$, with additional generation-dependent suppression from the Z_3 charges. For $\Lambda \sim 16 \text{ TeV}$, contributions to $K^0-\bar{K}^0$ mixing are estimated at the level of

$$|C_K| \sim \frac{\varepsilon^4}{\Lambda^2} \sim 10^{-12} \text{ GeV}^{-2}, \quad (36)$$

safely below the current experimental bound. Similarly, contributions to B -meson FCNCs and lepton flavour violation ($\mu \rightarrow e\gamma$) are highly suppressed.

The Belle II experiment has recently reported evidence for $B^+ \rightarrow K^+ \nu \bar{\nu}$ with a branching ratio $\sim 2.4\sigma$ above the SM prediction [17]. In the Z_3 framework, new-physics contributions to this mode would be further suppressed by the flavon scale and are not expected to produce observable deviations from the SM.

5.3 Precision tests

The most distinctive near-term tests of the Z_3 framework lie in improved determinations of quark mass ratios. The correlation (21) can be tested as lattice QCD and global fits reach percent-level precision on m_u/m_c and m_d/m_s independently. A future 100 TeV hadron collider could probe scalar resonances near $\Lambda \sim 10\text{--}20$ TeV, and observation of a scalar with flavour-non-universal couplings would provide a direct test of the FN mechanism.

On the neutrino side, experiments such as DUNE and Hyper-Kamiokande will further sharpen the determination of θ_{23} and δ_{CP} . The large mixing observed is already decisive evidence against a single-parameter Z_3 FN explanation for neutrino flavour, but precision measurements will guide the construction of viable alternatives.

6 Conclusions

We have analysed a minimal Z_3 Froggatt–Nielsen model of flavour and confronted it with the full set of quark and lepton data. Our main findings can be summarised as follows.

- The Z_3 column texture, with right-handed charges $(2, 1, 0)$ and a single expansion parameter $\varepsilon \simeq 0.015$, provides a *structural explanation* of the hierarchical fermion mass pattern. The scaling $m_1/m_2 \sim \varepsilon$, $m_1/m_3 \sim \varepsilon^2$ is a genuine prediction that holds for generic $\mathcal{O}(1)$ coefficients, as confirmed by a Monte Carlo scan over 10^5 random coefficient sets.
- The CKM mixing angles can be *accommodated* with $\mathcal{O}(1)$ coefficients ($\chi^2/\text{dof} \simeq 1.6$), but their hierarchical pattern is not a structural output of the Z_3 symmetry. This limitation is intrinsic to the column texture arising from uncharged left-handed doublets.
- The charged lepton masses are compatible with the same framework and expansion parameter.
- When applied to neutrinos within a type-I seesaw, the Z_3 framework fails decisively on two fronts. The mass spectrum is far too hierarchical: $m_1 : m_2 : m_3 \sim \varepsilon^4 : \varepsilon^2 : 1$ gives $\Delta m_{21}^2/\Delta m_{31}^2 \lesssim 10^{-4}$, at least two orders of magnitude below the observed ratio of 0.030. The PMNS mixing angles are generically $\mathcal{O}(1)$ random unitaries, providing no mechanism to predict the observed pattern. When M_R carries the Z_3 charge structure dictated by the correct Majorana charge algebra, the mass spectrum failure deepens to a suppression of eight orders of magnitude through a pseudo-Dirac mechanism.
- The failure is structural and independent of parameter choices: it stems from the single expansion parameter $\varepsilon = 0.015$ required by quark hierarchies, which enforces a neutrino mass spectrum that is far too hierarchical, and from the column texture, which leaves the PMNS angles as unstructured random rotations.

These results point toward a sectorial view of flavour. Simple cyclic symmetries such as Z_3 can elegantly account for the hierarchical pattern of fermion masses through the FN mechanism. However, the same mechanism is inherently incapable of generating the observed neutrino mass spectrum or providing structure to the PMNS mixing. This provides a sharp, quantitative motivation for introducing non-abelian discrete symmetries—at minimum A_4 , which can accommodate both neutrino masses and large mixing through its triplet representation—specifically for the lepton sector.

From a methodological perspective, our work illustrates the value of pushing simple flavour models to their limits and identifying precisely where they fail. The column texture’s success for mass ratios but failure for CKM hierarchy, and the complete failure for neutrino masses and mixing, provide a detailed map of the boundary between what Z_3 can and cannot explain. The quark sector needs only a mass hierarchy, which ε provides; the neutrino sector needs both a mild mass hierarchy and specific large mixing, and Z_3 provides neither. Such boundary-finding guides the construction of more sophisticated frameworks.

Declaration of generative AI and AI-assisted technologies in the manuscript preparation process

During the preparation of this work the author used Claude (Anthropic) in order to assist with numerical computations, Monte Carlo scan implementation, analytical cross-checks, and manuscript drafting. After using this tool, the author reviewed and edited all content, verified all physics independently, and takes full responsibility for the content of the published article.

References

- [1] C. D. Froggatt and H. B. Nielsen, “Hierarchy of Quark Masses, Cabibbo Angles and CP Violation,” Nucl. Phys. B **147** (1979) 277, doi:10.1016/0550-3213(79)90316-X.
- [2] G. G. Ross and M. Serna, “Unification and fermion mass structure,” Phys. Lett. B **664** (2008) 97, [arXiv:0704.1248 [hep-ph]].
- [3] G. Altarelli and F. Feruglio, “Discrete Flavor Symmetries and Models of Neutrino Mixing,” Rev. Mod. Phys. **82** (2010) 2701, [arXiv:1002.0211 [hep-ph]].
- [4] H. Ishimori, T. Kobayashi, H. Ohki, Y. Shimizu, H. Okada and M. Tanimoto, “Non-Abelian Discrete Symmetries in Particle Physics,” Prog. Theor. Phys. Suppl. **183** (2010) 1, [arXiv:1003.3552 [hep-th]].
- [5] S. F. King and C. Luhn, “Neutrino Mass and Mixing with Discrete Symmetry,” Rept. Prog. Phys. **76** (2013) 056201, [arXiv:1301.1340 [hep-ph]].
- [6] E. Ma and G. Rajasekaran, “Softly broken A4 symmetry for nearly degenerate neutrino masses,” Phys. Rev. D **64** (2001) 113012, [arXiv:hep-ph/0106291].
- [7] G. Altarelli and F. Feruglio, “Tri-bimaximal neutrino mixing from discrete symmetry,” Nucl. Phys. B **741** (2006) 215, [arXiv:hep-ph/0512103].
- [8] F. Bazzocchi, L. Merlo and S. Morisi, “Embedding A4 into left-right flavor symmetry,” JHEP **10** (2008) 063, [arXiv:0804.2110 [hep-ph]].
- [9] F. Feruglio, C. Hagedorn and R. Ziegler, “A realistic pattern of lepton mixing and masses from S4 and CP,” Eur. Phys. J. C **74** (2014) 2753, [arXiv:1303.7178 [hep-ph]].
- [10] S. F. King, T. Neder and A. J. Stuart, “Lepton mixing predictions from S4 in matter,” Phys. Lett. B **726** (2013) 312, [arXiv:1305.3200 [hep-ph]].
- [11] F. Feruglio, “Are neutrino masses modular forms?,” [arXiv:1706.08749 [hep-ph]].
- [12] T. Kobayashi, K. Tanaka and T. H. Tatsuishi, “Neutrino mixing from finite modular groups,” Phys. Rev. D **98** (2018) 016004, [arXiv:1803.10391 [hep-ph]].

- [13] J. T. Penedo and S. T. Petcov, “Lepton masses and mixing from modular S_4 symmetry,” Nucl. Phys. B **939** (2019) 292, [arXiv:1806.11040 [hep-ph]].
- [14] S. Aoki *et al.* [Flavour Lattice Averaging Group], “FLAG Review 2021,” Eur. Phys. J. C **82** (2022) 869, [arXiv:2111.09849 [hep-lat]].
- [15] S. Navas *et al.* [Particle Data Group], “Review of Particle Physics,” Phys. Rev. D **110** (2024) 030001.
- [16] I. Esteban, M. C. Gonzalez-Garcia, M. Maltoni, T. Schwetz and A. Zhou, “NuFit-6.0: updated global analysis of three-flavor neutrino oscillations,” JHEP **12** (2024) 216, [arXiv:2408.15088 [hep-ph]].
- [17] F. Abudinén *et al.* [Belle II], “Evidence for $B^+ \rightarrow K^+ \nu \bar{\nu}$ decay,” [arXiv:2311.14647 [hep-ex]].
- [18] A. de Gouvea and H. Murayama, “Neutrino mixing anarchy: Alive and kicking,” Phys. Lett. B **747** (2015) 479, [arXiv:1204.1249 [hep-ph]].